

# Thermal Reactions of Methanethiol and Ethanethiol on Si(100)

Ying-Huang Lai and Chuin-Tih Yeh

Department of Chemistry, National Tsing Hua University, Hsinchu 300, Taiwan

Chun-Chuan Yeh and Wei-Hsiu Hung\*

Department of Chemistry, National Taiwan Normal University, Taipei 116, Taiwan,  
National Synchrotron Radiation Research Center, Hsinchu 300, Taiwan

Received: November 14, 2002; In Final Form: June 2, 2003

We investigated adsorption and thermal decomposition of methanethiol ( $\text{CH}_3\text{SH}$ ) and ethanethiol ( $\text{C}_2\text{H}_5\text{SH}$ ) on a Si(100) surface by means of temperature-programmed desorption (TPD) and X-ray photoelectron spectroscopy (XPS) with synchrotron radiation. At an adsorption temperature of 115 K,  $\text{CH}_3\text{SH}$  and  $\text{C}_2\text{H}_5\text{SH}$  dissociate to form thiolates and hydrogen at a small coverage ( $<0.2$  monolayer), whereas molecular chemisorption occurs at a greater coverage; all chemisorbed molecules either deprotonate to form thiolate or desorb intact up to 400 K. Adsorption and decomposition of thiols occur on the dangling bonds of a dimer without breaking the Si–Si dimer bond, resulting in preservation of a  $2 \times 1$  LEED pattern. Thiolates further decompose to evolve hydrocarbons via scission of the C–S bond to form a sulfur adatom on the surface at a temperature above 550 K. Maximum desorption of surface sulfur as SiS occurs at 820 K.  $\text{CH}_3$  generated from  $\text{CH}_3\text{S}$  reacts with surface hydrogen to evolve  $\text{CH}_4$ , whereas the  $\text{C}_2\text{H}_5$  moiety of  $\text{C}_2\text{H}_5\text{S}$  undergoes  $\beta$ -hydride elimination to form  $\text{C}_2\text{H}_4$ . To a small extent, the alkyl moiety transfers onto the surface and undergoes dehydrogenation, resulting in desorption of hydrogen and deposition of carbon on the surface.

## Introduction

Reactions to modify a surface are important not only for engineering of surface energy and composition but also for attaching molecules with varied physical and chemical properties.<sup>1,2</sup> A number of studies have reported deposition of self-assembled monolayers (SAM) formed from organosulfur compounds via bonding of the sulfur atom to various surfaces; surfaces of noble metals such as Au and Ag have been much investigated.<sup>3,4</sup> Like adsorption of alkanethiols that occurs on noble metals, a SAM film might be prepared on a Si surface that can modify the chemical and physical properties of that surface and become potentially adaptable for such applications as protecting and insulating layers.<sup>5–7</sup> Organic monolayers with known orientation and controllable properties on a semiconductor surface have prospective applications as bio- or chemical sensors, and as molecular electronic and optoelectronic devices.<sup>8,9</sup> Organic/bio-molecules containing a sulfhydryl group ( $-\text{SH}$ ) have been attached to a Si surface with the sulfur atom as the tether.<sup>10,11</sup> The chemical behavior of thiols on a silicon surface is thus fundamentally important in the field of molecular electronics and has relevance to fields as diverse as biological science.

We report here an investigation of the mechanism of adsorption and decomposition of alkanethiols on a Si(100) surface, utilizing temperature-programmed desorption (TPD) and X-ray photoelectron spectroscopy (XPS); such spectral examination elucidates pathways of this surface reaction. In principle, the length of the carbon chain of an alkanethiol might exert a significant influence on the thermal stability and reaction mechanism due to the presence of  $\beta$ -hydrogen and the inter-

action between a Si surface and an alkyl group. We thus undertook a comparison of thermal reactivity and reaction products for alkanethiols with varied lengths of alkyl chain (i.e., RSH with  $\text{R}=\text{CH}_3$  and  $\text{C}_2\text{H}_5$ ), thus probing the formation and thermal stability of an alkanethiolate adlayer on the Si surface.

## Experimental Section

Experiments were performed in an ultrahigh vacuum (UHV) chamber with a base pressure  $2 \times 10^{-10}$  Torr. The system was equipped with a quadrupole mass filter (EPIC, Hiden), low-energy electron diffraction (LEED), and an electron-energy analyzer (HA100, VSW). The Si(100) samples (n-type,  $1-10 \Omega \cdot \text{cm}$ ) for our work had thickness 0.3 mm. To eliminate possible organic residues, the Si surface was cleaned with acetone, methanol, and hot  $\text{HNO}_3$  solution (1 M) in a sequence, and was followed by rinsing with distilled water. A Ta strip (thickness 0.025 mm) was uniformly pressed between two Si samples by Ta foils at two ends, which were in turn mounted on a copper block. The sample could be cooled to 115 K with liquid nitrogen via conduction through the copper block, and heated by resistive heating of the Ta strip and the Si sample. The sample temperature was monitored with a K-type thermocouple spot-welded onto a thin Ta foil that was inserted between the two Si samples. The Si surface was initially cleaned by means of resistive heating in situ slowly to 1200 K. After each experimental run, the surface was cleaned through  $\text{Ar}^+$  ion sputtering and annealed to 1200–1300 K; according to LEED, the surface then exhibited sharp  $2 \times 1$  and dim  $c(4 \times 2)$  patterns revealing two domains.<sup>12</sup> The cleanliness of the Si surface was verified with XPS measurements. To diminish effects of surface damage caused by ion sputtering we replaced Si samples after 3–4 experimental runs.

\* Corresponding author. Fax: +886-3-5789016. E-mail: hung@src.gov.tw.

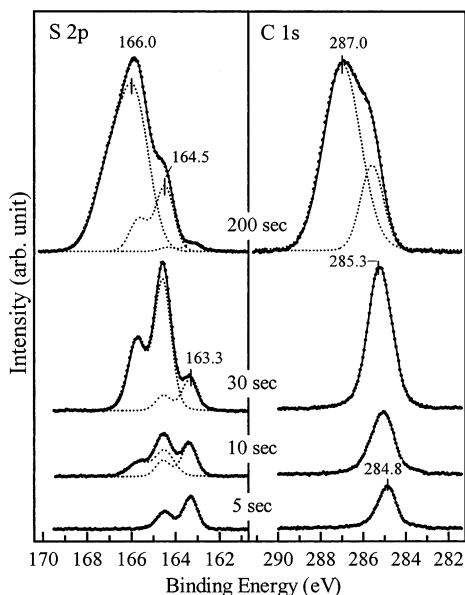


**Figure 1.** XPS spectra of S 2p and C 1s recorded for a Si surface with varied duration of exposure to  $\text{CH}_3\text{SH}$  at 115 K. Dots represent data collected after background subtraction; solid lines are fitted curves, and various components are shown in dashed lines. The photon energy used to collect these spectra is 400 eV.

Before use,  $\text{C}_2\text{H}_5\text{SH}$  (>99%, Merck) and  $\text{C}_4\text{H}_9\text{SH}$  (>98%, Merck) liquids were subjected to several freeze–pump–thaw cycles.  $\text{CH}_3\text{SH}$  (>99.5%, Matheson) was used without further purification. Alkanethiols were introduced onto the Si surface via a stainless steel tube with a pinhole (diameter 250  $\mu\text{m}$ ). During dosing, partial pressures of alkanethiols were controlled at  $2 \times 10^{-9}$  Torr and the sample surface was placed  $\sim 20$  mm in front of the doser pinhole to minimize contamination of the UHV system with thiols.

XPS were measured at the wide-range and LSGM beamlines of SRRC (Synchrotron Radiation Research Center, Taiwan); the angle of incidence of photons was  $45^\circ$  from the surface normal. Emitted photoelectrons were collected with an electron analyzer at an angle  $10^\circ$  from the surface normal in an angle-integrated mode. Collected spectra were numerically fitted with a Gaussian-broadened Lorentzian function after Shirley background subtraction with a third-order polynomial to each side of the feature. The Si and S 2p spectra were fitted with a branching ratio  $0.5 \pm 0.02$  between  $p_{1/2}$  and  $p_{3/2}$ ; the spin–orbit splittings were 0.60 and 1.18 eV, respectively. The onset of photoemission from an Au foil attached to the sample holder served as the Fermi level, corresponding to zero binding energy.

A quadrupole mass filter served for analysis of desorption products in the TPD measurement. The mass analyzer was enclosed in a differentially pumped cylinder, at the end of which is a skimmer with an entrance aperture (diameter 2 mm). For TPD measurement, the sample surface was placed about 2 mm before the aperture and in line of sight of the ionizer of the mass spectrometer; TPD scans were recorded on ramping the sample at a linear rate  $\sim 2$  K/s.

## Results and Discussion

Surface species upon adsorption and thermal fragmentation of  $\text{CH}_3\text{SH}$  on a Si surface were identified chemically using XPS measurement. Figure 1 shows spectra in S 2p and C 1s regions collected from a Si(100) surface exposed to  $\text{CH}_3\text{SH}$  at 115 K for varied duration. After brief exposure (5 s), only an S 2p spin–orbit doublet is observed with the  $p_{3/2}$  binding energy at

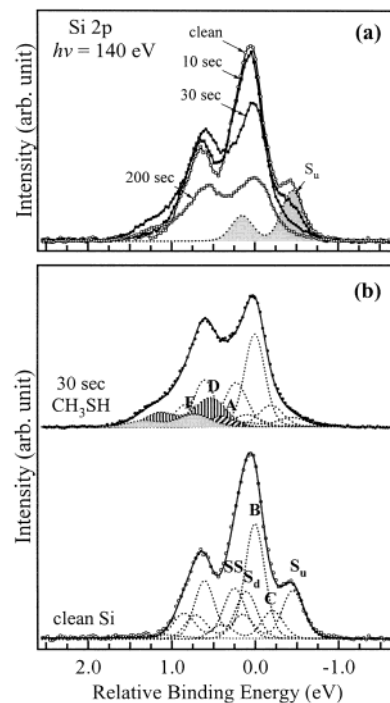


**Figure 2.** (a) XPS spectra of Si 2p recorded for a Si surface with varied duration of exposure to  $\text{CH}_3\text{SH}$  at 115 K; (b) decomposition of Si spectra from a clean surface and a surface exposed to  $\text{CH}_3\text{SH}$  for 30 s.

163.3 eV, which is attributed to surface methyl thiolate ( $\text{CH}_3\text{S}$ ) and discussed further below. Two additional S 2p $_{3/2}$  components at 164.5 and 166.0 eV develop with increasing duration of exposure. The intensity of the former component reaches a maximum at an exposure of duration  $\sim 30$  s, whereas the intensity of the latter component does not saturate upon extended exposure of  $\text{CH}_3\text{SH}$ . These S 2p $_{3/2}$  components are thus assigned to  $\text{CH}_3\text{SH}$  molecules chemisorbed and physisorbed on the surface, respectively.

XPS data indicate that on initial adsorption  $\text{CH}_3\text{SH}$  molecules dissociate to form surface  $\text{CH}_3\text{S}$  and hydrogen ( $\text{CH}_3\text{SH} \rightarrow \text{CH}_3\text{S} + \text{H}$ ).  $\text{CH}_3\text{SH}$  can also adsorb molecularly on the surface at large coverage with increasing coverage of  $\text{CH}_3\text{S}$ . For a saturated monolayer, 15–20% of adsorbed  $\text{CH}_3\text{SH}$  deprotonates to form thiolate at adsorption temperature 115 K.  $\text{CH}_3\text{SH}$  molecules can condense on the surface after adsorption sites become saturated, but the sticking coefficient is greatly decreased. Parallel to these S 2p spectra, corresponding C 1s chemical states of methyl groups have 1s binding energies at 285.3 and 287.0 eV. The former feature is assigned to dissociative  $\text{CH}_3\text{S}$  and chemisorbed  $\text{CH}_3\text{SH}$ , and the latter feature is due to physisorbed  $\text{CH}_3\text{SH}$ . These assignments of XPS features are consistent with an observation that intensities of S 2p and C 1s signals due to chemisorbed  $\text{CH}_3\text{SH}$  and  $\text{CH}_3\text{S}$  become attenuated by physisorbed  $\text{CH}_3\text{SH}$  molecules on protracted exposure ( $> 30$  s).

Figure 2a shows core level spectra of Si 2p taken before and after a clean Si surface is exposed to  $\text{CH}_3\text{SH}$  at 115 K. The Si 2p binding energy is referred to the bulk 2p $_{3/2}$  component so that complication resulting from the variation of surface band bending can be eliminated after adsorption and thermal decomposition of  $\text{CH}_3\text{SH}$ . Without curve fitting, we find that Si 2p spectra show broadening at the side of greater binding energy because of interaction of the Si surface and  $\text{CH}_3\text{SH}$ . It is generally accepted that the Si 2p spectrum of a clean Si(100)– $2 \times 1$  surface is fitted with four surface components ( $S_u$ ,  $S_d$ ,  $SS$ , and  $C$ ) with the bulk component ( $B$ ) as shown in Figure 2b;

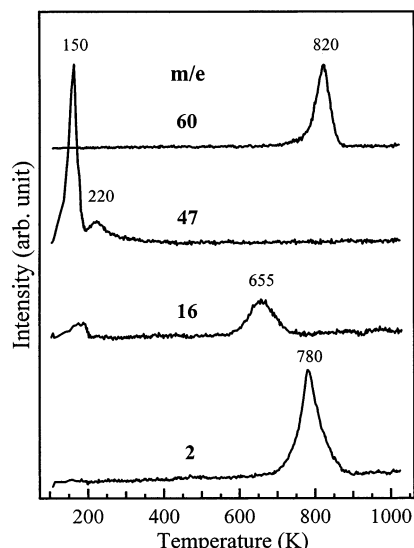


**Figure 3.** Composite temperature-programmed desorption scans collected from a Si(100) surface exposed to  $\text{CH}_3\text{SH}$  at 115 K for 200 s.

components  $S_u$  and  $S_d$  correspond to upward and downward buckled Si atoms of asymmetric dimers, respectively; component SS is assigned to the second layer Si atoms, and component C is likely due to third-layer Si atoms or defects.<sup>13–15</sup> The energy shifts relative to the bulk component are  $-0.46$ ,  $-0.21$ ,  $0.09$ , and  $0.25$  eV, respectively, in agreement with previous results except for a small difference in the energy shifts.

For simplicity and clarity, only the upward buckled Si of a dimer at  $-0.46$  eV for the clean surface is shown in Figure 2a. This component is gradually attenuated upon increasing exposure of  $\text{CH}_3\text{SH}$ , indicating that a reaction occurs between  $\text{CH}_3\text{SH}$  and surface Si atoms of dimers. The ordered  $(2 \times 1)$  LEED pattern is maintained after adsorption of  $\text{CH}_3\text{SH}$  at 115 K, although its intensity decreases. We assume that at 115 K the molecular  $\text{CH}_3\text{SH}$  and the dissociative H and  $\text{CH}_3\text{S}$  species are likely bound to existing dangling bonds of a Si dimer without major disruption of Si surface structure. As shown in Figure 2b, taken from a Si surface exposed to  $\text{CH}_3\text{SH}$  for 30 s, the four surface components of Si 2p decrease in intensity and three new Si 2p components (labeled as components A, D, and E) appear at the side of large binding energy with energy shifts 0.42, 0.53, and 0.70 eV relative to the bulk component. As mentioned above, dissociation of  $\text{CH}_3\text{S-H}$  produces surface hydrogen and  $\text{CH}_3\text{S}$ . On the basis of infrared reflection spectroscopy, it has been reported that  $\text{CH}_3\text{OH}$  dissociates to form surface  $\text{Si-OCH}_3$  and  $\text{Si-H}$  without breaking the  $\text{Si-Si}$  dimer bond at 150 K. The  $\text{Si-H}$  species resulting from dissociation of  $\text{CH}_3\text{O-H}$  has a chemical shift of Si 2p at 0.435 eV with respect to the bulk Si.<sup>15</sup> Thus, component A is assigned to surface Si bonded to hydrogen. Components D and E at large binding energy are assigned to surface Si atoms of a dimer bonded to molecular  $\text{CH}_3\text{SH}$  and dissociative  $\text{CH}_3\text{S}$  via electron-withdrawing S atoms, respectively.

Figure 3 shows TPD scans for a Si(100) surface exposed to  $\text{CH}_3\text{SH}$  at 115 K for 200 s. To detect possible products evolving during thermal decomposition of  $\text{CH}_3\text{SH}$  on the surface, we observed several possible fragments. Desorption features of molecular  $\text{CH}_3\text{SH}$  ( $m/e = 47$ ) are observed at 150 and 220 K, and are attributed to desorption of physisorbed and chemisorbed  $\text{CH}_3\text{SH}$ . Most chemisorbed  $\text{CH}_3\text{SH}$  undergoes thermal decomposition, resulting in desorption of hydrogen ( $m/e = 2$ ),  $\text{CH}_4$  ( $m/e = 16$ ), and  $\text{SiS}$  ( $m/e = 60$ ). Desorption of hydrogen results in an intense feature at 780 K and resembles the  $\beta_1$  states of

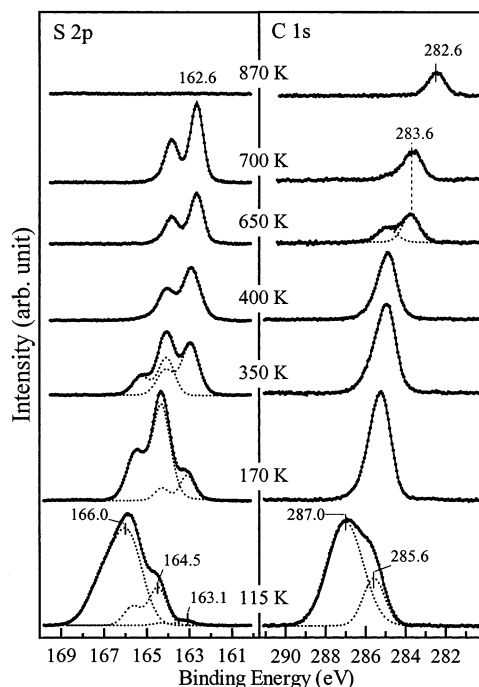


**Figure 4.** XPS spectra of S 2p and C 1s for a Si(100) surface exposed to  $\text{CH}_3\text{SH}$  for 200 s at 115 K and subsequently heated to the indicated temperatures. The photon energy used to collect these spectra is 400 eV.

hydrogen desorption observed after adsorption of atomic hydrogen on Si(100), which are attributed to recombination of surface hydrogen in a form of Si monohydride.<sup>16</sup> Maximum desorption of  $\text{CH}_4$  occurs at 655 K, due to the hydrogenation of  $\text{CH}_3$  moiety. Formation of  $\text{C}_2\text{H}_6$  via coupling of  $\text{CH}_3$  groups of  $\text{CH}_3\text{SH}$  is not observed, unlike the case of transition metals.<sup>17</sup> Desorption of  $\text{SiS}$  is observed with a feature at 820 K, as observed for adsorption of elemental sulfur and  $\text{H}_2\text{S}$  on a Si surface.<sup>18,19</sup> Hence, for the decomposition of  $\text{CH}_3\text{SH}$ ,  $\text{SiS}$  is desorbed via formation of atomic sulfur on a Si surface.

The thermal evolution of XPS spectra is used to characterize the variation of surface composition during thermal decomposition of  $\text{CH}_3\text{SH}$  on a Si surface and correlates with TPD results to elucidate the reaction intermediates. Figures 4 and 5 show core-level spectra of S 2p, C 1s, and Si 2p obtained from a Si(100) surface that is exposed to  $\text{CH}_3\text{SH}$  at 115 K for 200 s, then warmed to the indicated temperatures. All XPS spectra were recorded for samples at 115 K after the sample was heated to a desired temperature at a linear rate  $\sim 1$  K/s and cooled immediately on abrupt termination of heating. The S  $2p_{3/2}$  (166.0 eV) and C 1s (287.0 eV) features due to physisorbed  $\text{CH}_3\text{SH}$  disappear upon heating the sample to 170 K. Between 170 and 400 K, the S 2p peak assigned to  $\text{CH}_3\text{S}$  gradually increases, whereas the S  $2p_{3/2}$  peak at 164.5 eV due to chemisorbed  $\text{CH}_3\text{SH}$  decreases. Thermal dissociation of chemisorbed  $\text{CH}_3\text{SH}$  occurs to form  $\text{CH}_3\text{S}$  in this temperature range. In addition, the total integrated area of S 2p decreases because a proportion of chemisorbed  $\text{CH}_3\text{SH}$  is desorbed intact as shown in TPD data.

A previous study of infrared reflection spectroscopy showed that all chemisorbed  $\text{CH}_3\text{OH}$  molecules dissociate to form surface hydrogen and methoxy species ( $\text{CH}_3\text{O}$ ) on Si(100)- $2 \times 1$  at 150 K.<sup>20</sup> Our XPS results show that the dissociation temperature of chemisorbed  $\text{CH}_3\text{S-H}$  is higher than that of  $\text{CH}_3\text{O-H}$ , although the bond strength of  $\text{S-H}$  (80 kcal/mol) is less than that of  $\text{O-H}$  (102 kcal/mol).<sup>21</sup> Thus, we propose that the dissociation temperatures of  $\text{CH}_3\text{S-H}$  and  $\text{CH}_3\text{O-H}$  on Si-



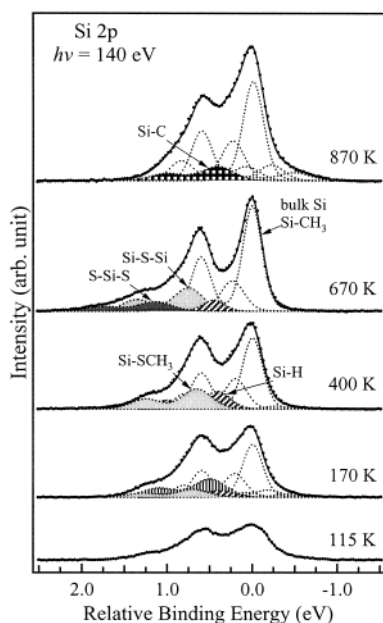


**Figure 5.** XPS spectra of Si 2p for a Si(100) surface exposed to CH<sub>3</sub>SH for 200 s at 115 K and subsequently heated to the indicated temperatures. The photon energy used to collect these spectra is 140 eV.

(100) are mainly determined by the formation of Si–S (148 kcal/mol) and Si–O (190 kcal/mol) bonds, respectively. On the other hand, the dissociative adsorption of both CH<sub>3</sub>SH and CH<sub>3</sub>OH molecules do not break the Si–Si dimer bond and preserve the 2 × 1 surface pattern.<sup>15</sup>

Upon annealing the sample above 650 K, the S 2p spin-orbit doublets (*p*<sub>1/2</sub> and *p*<sub>3/2</sub>) become better resolved (having a smaller fwhm) and shift slightly to smaller binding energy. This behavior reflects that CH<sub>3</sub>S further decomposes to form sulfur adatom (*S*<sub>(ad)</sub>) and liberates the CH<sub>3</sub> group via breaking the CH<sub>3</sub>–S bond. A new C 1s feature that appears at 283.6 eV is thus assigned to surface CH<sub>3</sub>.<sup>22</sup> As shown in Figure 3, desorption of CH<sub>4</sub> is observed in this temperature range and corresponds to the decreasing total intensity of C 1s. CH<sub>4</sub> is formed via reaction between the CH<sub>3</sub> moiety and surface hydrogen that originates from the dissociation of CH<sub>3</sub>S–H at low temperature. We thus conclude that the CH<sub>3</sub> moiety generated on breaking the CH<sub>3</sub>–S bond either transfers onto the surface or hydrogenates to desorb as CH<sub>4</sub>.

At 700 K, all CH<sub>3</sub>S species dissociate completely to form sulfur adatoms and leave a portion of the CH<sub>3</sub> moiety on the surface. The intensity of S 2p increases significantly after decomposition of CH<sub>3</sub>S. Because the CH<sub>3</sub> group is liberated from the sulfur atom after decomposition of CH<sub>3</sub>S, the scattering of photoelectrons emitted from S 2p by the CH<sub>3</sub> moiety is diminished and the intensity of S 2p in XPS measurements thus increases. Between 650 and 870 K, the C 1s feature shifts down toward 282.6 eV. Previous observations of vibrational spectra indicated that surface CH<sub>3</sub> on a Si surface dissociates to form SiH near 700 K.<sup>23–26</sup> We thus attribute this C 1s peak to surface carbon that results from dehydrogenation of surface CH<sub>3</sub>.<sup>27,28</sup> Surface hydrogen is also formed during dehydrogenation of CH<sub>3</sub> and is subsequently desorbed with an intense feature at 780 K, as shown in Figure 3.<sup>29</sup> The S 2p peak disappears in this temperature range because sulfur is removed from the surface with a maximum effect at 820 K as shown in TPD data.

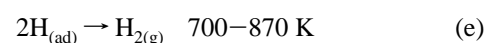
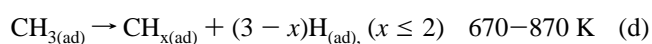
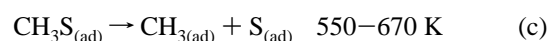
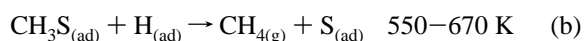
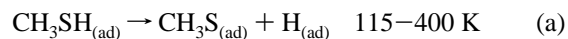
Figure 5 shows Si 2p core-level spectra as a function of temperature. A surface exposed to CH<sub>3</sub>SH at 115 K for 200 s is covered with chemisorbed and physisorbed CH<sub>3</sub>SH. Upon

heating to 170 K, the spectral intensity of Si 2p becomes higher because of desorption of physisorbed CH<sub>3</sub>SH, and the decomposition of the Si 2p spectrum is similar to that observed for a Si surface exposed to CH<sub>3</sub>SH at 115 K for 30 s as shown in Figure 2b, for a surface saturated with chemisorbed CH<sub>3</sub>SH and dissociative CH<sub>3</sub>S. At 400 K, chemisorbed CH<sub>3</sub>SH decomposes completely into surface CH<sub>3</sub>S and H, and the Si 2p spectra are thus fitted with two components with chemical shifts at 0.41 and 0.67 eV due to Si–H and Si–SCH<sub>3</sub>, respectively, as shown in Figure 4.

At 670 K, the CH<sub>3</sub>S species decomposes further into surface sulfur and desorbs as CH<sub>4</sub> or forms surface CH<sub>3</sub> via cleavage of the CH<sub>3</sub>–S bond. Decomposition of the Si spectrum yields two S–induced Si 2p components at 0.75 and 1.15 eV attributed to surface Si bound to sulfur atoms with oxidation states +1 and +2, respectively. Theoretical work indicates that a surface S atom absorbs at a bridge position above the topmost Si atoms, as the most energetically stable conformation.<sup>30</sup> Accordingly, we propose that the S–induced Si peak at 0.75 eV is due to surface Si atoms bound to bridge-bonded sulfur (Si–S–Si). Formation of Si–S–Si might occur on Si atoms of a dimer on breaking the Si–Si bond or with Si atoms between two Si dimers. According to the LEED observation, the 2 × 1 pattern persists after the Si surface exposed to CH<sub>3</sub>SH at 115 K is heated to 670 K, although its intensity becomes small. Hence, adsorption and decomposition of CH<sub>3</sub>SH might occur on dangling bonds of a Si dimer without breaking the Si–Si bond of that dimer. Thus, the Si–S–Si species is proposed to be formed mainly on two Si atoms of adjacent dimers. The large chemical shift of Si 2p<sub>3/2</sub> at 1.15 eV is near that observed for Si(100)–1 × 1–S, for which the surface Si atom is terminated with bridge-bonded sulfur and has an oxidation state +2.<sup>31</sup> The Si 2p<sub>3/2</sub> component is thus attributed to a surface S–Si–S species that we propose to form from decomposition of two adjacent CH<sub>3</sub>S. The intensity ratio of the component at 0 eV to the second-layer Si is significantly greater than that of the bulk Si to the second-layer Si for a clean Si surface. On the basis of C 1s spectra shown in Figure 4, a portion of CH<sub>3</sub> groups liberated from dissociation of CH<sub>3</sub>S transfers onto the surface in this temperature range. Thus, the component at 0 eV is attributed to bulk Si and surface Si bonded to the CH<sub>3</sub> group (Si–CH<sub>3</sub>).

After annealing the sample to 870 K, the surface S is removed in a form of SiS and a well-defined 2 × 1 LEED pattern is recovered. However, a proportion of CH<sub>3</sub> moiety dehydrogenates to produce surface carbon. At 870 K, the Si 2p spectrum consists of a *p*<sub>3/2</sub> component with chemical shift at ~0.45 eV due to the SiC species, and four surface components as obtained for a clean Si surface.<sup>14</sup>

On the basis of TPD and XPS results, the mechanism of decomposition of CH<sub>3</sub>SH on Si(100) is summarized as follows:



Our XPS data indicate that thiolate species on the Si surface sustain up to 550 K and is more stable than those formed on transition metals. The dissociation temperature of the CH<sub>3</sub>–S

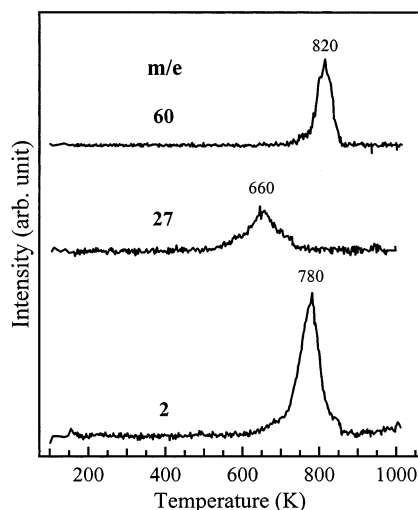


**Figure 6.** Composite temperature-programmed desorption scans collected from a Si(100) surface exposed to  $C_2H_5SH$  at 115 K for 30 s.

bond is less than that of  $CH_3-O$  by  $\sim 150$  K.<sup>32</sup>  $H_2$ ,  $CH_4$ , and  $SiS$  are products of desorption, and only carbon is left on the Si surface after decomposition of  $CH_3SH$  on annealing the sample to 870 K.

To understand the effect of length of alkyl chain on the reactions of thiols on a Si surface, we studied adsorption also of  $C_2H_5SH$ . Figure 6 shows TPD scans for a Si surface exposed to  $C_2H_5SH$  for 30 s.  $H_2$  ( $m/e = 2$ ) and  $C_2H_4$  ( $m/e = 27$ ) are desorption products of  $C_2H_5SH$  decomposition with maximum signals at 660 and 780 K, respectively. Desorption of  $C_2H_6$  ( $m/e = 30$ ), a hydrogenation product, is not observed. To avoid background interference from residual gas (e.g.,  $CO$  and  $N_2$ ) in the chamber, we recorded the intensity of a signal for  $C_2H_4$  desorption at  $m/e = 27$ , rather than at  $m/e = 28$ .  $C_2H_4$  is formed via  $\beta$ -hydride elimination of surface  $C_2H_5$  moiety of  $C_2H_5S$  ( $C_2H_5S \rightarrow C_2H_4 + H + S$ ), as generally observed for transition metals.<sup>33,34</sup> Dissociation of the  $C-H$  bond is catalyzed by the metallic surface to form metal-H species,<sup>33,35</sup> but the desorption temperature of  $C_2H_4$  is near that of  $CH_4$  obtained from decomposition of  $CH_3SH$ . Hence, the reaction of alkanethiolate on a Si surface seems to be determined by the cleavage of the  $C-S$  bond. This behavior is consistent with an observation that the temperature of dissociation of the  $CH_3-S$  bond is significantly less than that of  $CH_3-O$ , for which the bond energy of  $C-O$  is greater than that of  $C-S$ . Desorption of hydrogen with a maximum at 780 K reflects recombination of surface hydrogen produced on dissociation of the  $C_2H_5S-H$  bond and  $\beta$ -hydride elimination of  $C_2H_5$  groups. This observation is consistent with previous results with a  $C_2H_5$  group from  $C_2H_5Br$  adsorption on Si(100) proceeding through a  $\beta$ -elimination reaction on the surface to form  $C_2H_4$ .<sup>36-38</sup>

For a comparison of adsorption density of alkanethiols with varied lengths of alkyl chain, Figure 7 shows XPS spectra recorded for Si surfaces exposed to  $CH_3SH$ ,  $C_2H_5SH$ , and  $C_4H_9SH$  for 200 s at 115 K and subsequently heated to 170–200 K to remove physisorbed molecules. Assuming that the adsorption density of alkanethiol/ alkanethiolate is proportional to the ratio of S 2p-to-Si 2p intensity, we find that the ratio varies less than the chain length of an alkyl group. Hence, alkanethiols ( $CH_3SH$ ,  $C_2H_5SH$ , and  $C_4H_9SH$ ) adsorb on the Si surface with the alkyl group away from the surface, instead of lying on the surface. This deduction is consistent with an argument that dissociation of thiolate is determined by the  $C-S$  cleavage and

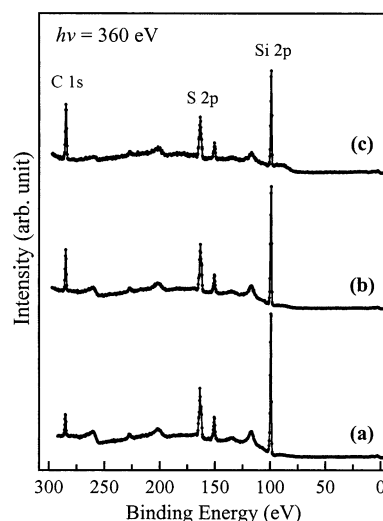


**Figure 7.** Comparison of XPS spectra recorded for Si surfaces exposed to (a)  $CH_3SH$ , (b)  $C_2H_5SH$ , and (c)  $C_4H_9SH$  for 200 s at 115 K and heated to  $\sim 170$ –200 K.

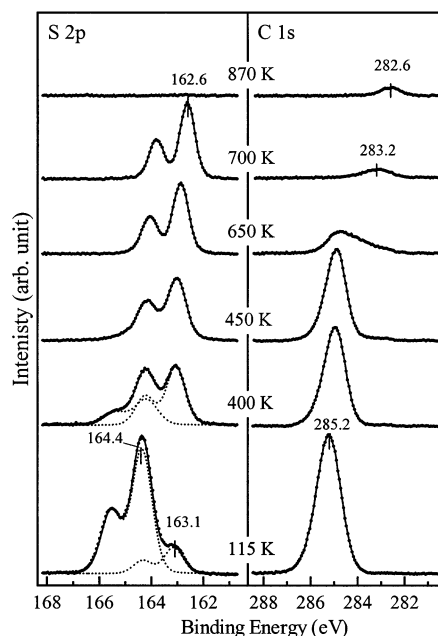


**Figure 8.** XPS spectra of S 2p and C 1s for a Si(100) surface exposed to  $C_2H_5SH$  for 30 s at 115 K and subsequently heated to the indicated temperatures.

is little affected by the interaction between the Si surface and an alkyl group as observed on a metallic surface.

Figure 8 shows S 2p and C 1s XPS spectra of a Si(100) surface exposed to  $C_2H_5SH$  at 115 K for 30 s, so that it became saturated with chemisorbed  $C_2H_5S$  and  $C_2H_5SH$ , as a function of surface temperature. The S 2p spectrum at 115 K contains two S 2p<sub>3/2</sub> features at 163.1 and 164.4 eV due to adsorbed  $C_2H_5SH$  and  $C_2H_5S$ .  $C_2H_5SH$  to a small proportion (15%) decomposes into  $C_2H_5S$  on the Si surface at the temperature of exposure, 115 K;  $C_2H_5SH$  seems slightly less reactive than  $CH_3SH$ . Between 170 and 450 K, the intensity of S 2p<sub>3/2</sub> at 162.4 eV gradually increases, indicating deprotonation of chemisorbed  $C_2H_5SH$ . Annealing the sample to 650 K causes a rapid decrease of C 1s intensity, accompanied by formation and desorption of  $C_2H_4$ . In addition, the spin-orbit doublet of S 2p becomes sharper, although its binding energy does not significantly alter. Consistent with TPD data,  $C_2H_5S$  decomposes to form surface sulfur and to desorb  $C_2H_4$  via a concerted mechanism of

breaking of the  $\text{C}_2\text{H}_5\text{—S}$  bond and  $\beta$ -hydride elimination. At 700 K, all  $\text{C}_2\text{H}_5\text{S}$  decomposes into surface sulfur. The C 1s feature becomes weaker and shifts to 283.2 eV, because a small proportion of  $\text{C}_2\text{H}_5$  moiety transfers onto the surface. At 870 K, surface sulfur is desorbed from the surface as SiS and the surface  $\text{C}_2\text{H}_5$  group dehydrogenates to form surface carbon with C 1s at 282.6 eV. The coverage of surface carbon remaining after decomposition of  $\text{C}_2\text{H}_5\text{SH}$  is less than for the case of  $\text{CH}_3\text{—SH}$ , indicating that most  $\text{C}_2\text{H}_5$  moieties undergo  $\beta$ -hydride elimination, rather than dehydrogenation.

## Conclusion

TPD results show that  $\text{H}_2$ ,  $\text{CH}_4$ , and SiS are desorbed from a Si surface during thermal decomposition of  $\text{CH}_3\text{SH}$ . XPS data indicate that dissociative adsorption of  $\text{CH}_3\text{SH}$  yields surface  $\text{CH}_3\text{S}$  and H on Si(100) at 400 K. The resulting  $\text{CH}_3\text{S}$  and H bind to dangling bonds without breaking the Si—Si bond of a dimer; the  $(2 \times 1)$  surface structure is consequently preserved. Surface  $\text{CH}_3\text{S}$  dissociates further to form Si—S—Si and S—Si—S intermediates at temperatures above 550 K. Si monohydride is proposed to be the surface intermediate, corresponding to desorption of hydrogen peaking at 780 K.  $\text{C}_2\text{H}_5\text{SH}$  shows similar behavior of adsorption and dissociation, although  $\text{C}_2\text{H}_5\text{SH}$  is slightly less reactive to deprotonation on the Si surface. At 550 K, decomposition of both  $\text{CH}_3\text{S}$  and  $\text{C}_2\text{H}_5\text{S}$  thiolates proceeds, to form surface S and to desorb  $\text{CH}_4$  and  $\text{C}_2\text{H}_4$ , respectively; the rate of this reaction is determined by breaking of the C—S bonds. Formation of  $\text{CH}_4$  results from reaction between surface H and the  $\text{CH}_3$  moiety of  $\text{CH}_3\text{S}$ , and desorption of  $\text{C}_2\text{H}_4$  occurs via  $\beta$ -hydride elimination of the  $\text{C}_2\text{H}_5$  moiety of  $\text{C}_2\text{H}_5\text{S}$ .

Our results provide information about the adsorption and thermal reaction of alkanethiol/alkanethiolate on a Si surface, when introduced onto the Si surface through vapor deposition in UHV conditions. As expected from reaction mechanisms of  $\text{CH}_3\text{SH}$  and  $\text{C}_2\text{H}_5\text{SH}$ , other thiol molecules with inert alkyl groups ( $\text{R—SH}$ ) can deprotonate and form a thiolate layer on heating to  $\sim 400$  K. The resulting thiolate is incorporated with surface hydrogen and can sustain up to  $\sim 550$  K, and might provide a passivation layer in the fabrication of electronic devices. This surface modification might extend potentially to immobilization of proteins and bio-molecules in the manufacture of biochips and biosensors, in which the thiol molecule with a second functional group, instead of the inert alkyl moiety, acts as a link to the Si surface via a covalent Si—S bond.

**Acknowledgment.** This work was supported by SRRC and the National Science Council under Grant No. NSC91-2113-M-213-003.

## References and Notes

- (1) Ulman, A. *Chem. Rev.* **1996**, 96, 1533.
- (2) Bent, S. F. *J. Phys. Chem. B* **2002**, 106, 2830.
- (3) Ulman, A. *An Introduction to Ultrathin Organic Films from Langmuir—Blodgett to Self-Assembly*; Academic Press: New York, 1991.
- (4) Nuzzo, G. R.; Fusco, R. A.; Allara, D. L. *J. Am. Chem. Soc.* **1987**, 109, 2358.
- (5) Linford, M. R.; Chidsey, C. E. D. *J. Am. Chem. Soc.* **1993**, 115, 12631.
- (6) Bansal, A.; Li, X.; Lauerman, I.; Lewis, N. S. *J. Am. Chem. Soc.* **1996**, 118, 7225.
- (7) Bergerson, W. F.; Mulder, J. A.; Hsung, R. P.; Zhu, X. Y. *J. Am. Chem. Soc.* **1999**, 121, 454.
- (8) Mui, C.; Wang, G. T.; Bent, S. F.; Musgrave, C. B. *J. Chem. Phys.* **2001**, 114, 10170.
- (9) Strother, T.; Hamers, R. J.; Smith, L. M. *Nucleic Acids Res.* **2000**, 28, 3535.
- (10) Crain, J. N.; Kirakosian, A.; Lin, J. L.; Gu, Y.; Shah, R. R.; Abott, N. L. *J. Appl. Phys.* **2001**, 90, 3291.
- (11) Coulter, S. K.; Schwartz, M. P.; Hamers, R. J. *J. Phys. Chem. B* **2001**, 105, 3079.
- (12) Kato, H.; Watanabe, K.; Matsumoto, Y. *Surf. Sci.* **1998**, 398, L297.
- (13) Landemark, E.; Karlsson, C. J.; Chao, Y. C.; Uhrberg, R. I. G. *Phys. Rev. Lett.* **1992**, 69, 1588.
- (14) Xu, S. H.; Yang, Y.; Keffe, M.; Lapeyre, G. *J. Phys. Rev. B* **1999**, 60, 11586.
- (15) Casaletto, M. P.; Znoni, R.; Carbone, M.; Piancastelli, M. N.; Aballe, L.; Weiss, W.; Horn, K. *Surf. Sci.* **2002**, 505, 251.
- (16) Waltenburg, H. N.; Yates, J. T., Jr. *Chem. Rev.* **1995**, 95, 1589.
- (17) Lai, Y. H.; Yeh, C. T.; Cheng, S. H.; Liao, P.; Hung, W. H. *J. Phys. Chem. B* **2002**, 106, 5438.
- (18) Papageorgopoulos, A.; Kamaratos, M. *Surf. Sci.* **1996**, 352–354, 364.
- (19) Lai, Y. H.; Yeh, C. T.; Lin, Y. H.; Hung, W. H. *Surf. Sci.* **2002**, 519, 150.
- (20) Ehrley, W.; Butz, R.; Mantl S. *Surf. Sci.* **1991**, 248, 193.
- (21) Lide, D. R. *CRC Handbook of Chemistry and Physics*, 82nd ed.; CRC Press: Boca Raton, FL, 2001–2002.
- (22) Bu, Y.; D. Shinn, W.; Lin, M. C. *Surf. Sci.* **1992**, 276, 184.
- (23) Kong, M. J.; Lee, S. S.; Lyubovitsky, J.; Bent, S. F. *Chem. Phys. Lett.* **1996**, 263, 1.
- (24) Colaianni, M. L.; Chen, P. J.; Gutleben, H.; Yates, J. T., Jr. *Chem. Phys. Lett.* **1992**, 191, 561.
- (25) Rueter, M. A.; Vohs, J. M. *J. Vac. Sci. Technol. A* **1991**, 9, 2916.
- (26) Brown, K. A.; Ho, W. *Surf. Sci.* **1995**, 338, 111.
- (27) Rochet, F.; Jolly, F.; Bournel, F.; Dufour, G.; Sirotti, F.; Cantin, J. L. *Phys. Rev. B* **1998**, 58, 11029.
- (28) Ikeda, M.; Maruoka, T.; Nagashima, N. *Surf. Sci.* **1998**, 416, 240.
- (29) Gutleben, H.; Lucs, S. R.; Cheng, C. C.; Choyke, W. J.; Yates, J. T., Jr. *Surf. Sci.* **1991**, 257, 145.
- (30) Kruger, P.; Pollmann, J. *Phys. Rev. B* **1993**, 47, 1898.
- (31) Roche, J.; Ryan, P.; Hughes, G. *Surf. Sci.* **2000**, 465, 115.
- (32) Edamoto, K.; Kubota, Y.; Onchi, M.; Nishijima, M. *Surf. Sci.* **1984**, 146, L533.
- (33) Bent, B. E. *Chem. Rev.* **1996**, 96, 1361.
- (34) Chiang, C. M.; Wenzlaff, H.; Jenks, C. J.; Bent, B. E. *J. Vac. Sci. Technol. A* **1992**, 10, 2185.
- (35) Zaera, F. *Chem. Rev.* **1995**, 95, 2651.
- (36) Klug, D. A.; Greenlief, C. M. *J. Vac. Sci. Technol. A* **1996**, 14, 1826.
- (37) Koleske, D. D.; Gates, S. M. *J. Phys. Chem.* **1993**, 99, 5091.
- (38) Sampson, G. M.; White, J. M.; Ekerdt, J. G. *Surf. Sci.* **1998**, 411, 163.